© 2018. Published by The Company of Biologists Ltd | Journal of Cell Science (2018) 131, jcs215335. doi:10.1242/jcs.215335

RESEARCH ARTICLE

Golgi localization of oxysterol binding protein-related protein 4L (ORP4L) is regulated by ligand binding

Antonietta Pietrangelo and Neale D. Ridgway*

ABSTRACT

Oxysterol binding protein (OSBP)-related protein 4L (ORP4L, also known as OSBPL2), a closely related paralogue and interacting partner of OSBP, binds sterols and phosphatidylinositol 4-phosphate [PI(4)P] and regulates cell proliferative signalling at the plasma membrane (PM). Here, we report that ORP4L also interacts with the *trans*-Golgi network (TGN) in an OSBP-, sterol- and PI(4)P-dependent manner. Characterization of ORP4L lipid and VAP binding mutants indicated an indirect mechanism for translocation to ER–Golgi contact sites in response to 25-hydroxycholesterol that was dependent on OSBP and PI(4)P. shRNA silencing revealed that ORP4L was required to maintain the organization and PI(4)P content of the Golgi and TGN. In contrast, the interaction of ORP4L with the PM was not dependent on its sterol, PI(4)P or VAP binding activities. At the PM, ORP4L partially localized with a genetically encoded probe for PI(4)P but not with a probe for phosphatidylinositol 4,5-bisphosphate. We conclude that ORP4L is differentially localized to the PM and ER–Golgi contacts sites. OSBP-, lipid- and VAP-regulated interactions of ORP4L with ER–Golgi contact sites are involved in the maintenance of Golgi and TGN structure.

KEY WORDS: Oxysterol binding proteins, Golgi complex, Membrane contact sites, Phosphatidylinositol 4-phosphate

INTRODUCTION

The endoplasmic reticulum (ER) is the major site for synthesis of lipids and cholesterol, which are subsequently distributed to other organelles by vesicular transport or lipid transfer proteins (LTPs) that shield the ligand from the aqueous environment during transport. Many LTP families have been identified with potential lipid transfer, signalling or presentation functions (reviewed in Wong et al., 2017). Oxysterol binding protein (OSBP) and related proteins (ORPs) constitute a 12-gene family of mammalian lipid transport and regulatory proteins typified by a conserved C-terminal lipid binding OSBP homology domain (OHD) (Ngo et al., 2010; Olkkonen and Li, 2013). Additional N-terminal pleckstrin homology (PH), two phenylalanines in an acidic tract (FFAT) and ankyrin domains confer context to the lipid transfer and regulatory activities of OSBP and ORPs by promoting their localization to membrane contact sites (MCSs) between organelles. For example, ORP1L regulates endosome positioning and cholesterol transport at late endosome–ER contacts (van der Kant et al., 2013; Zhao and Ridgway, 2017), ORP5 and ORP8 transport phosphatidylserine and phosphatidylinositol phosphates at ER–plasma membrane (PM) contacts (Chung et al., 2015; Ghai et al., 2017), and ORP2 regulates TAG metabolism at lipid droplets (Jansen et al., 2011).

The OHD of OSBP was originally shown to bind cholesterol and oxysterol derivatives (Dawson et al., 1989; Wang et al., 2008). However, a feature of all OSBP family members is a conserved di-histidine motif in the OHD that is necessary for binding phosphatidylinositol 4-phosphate [PI(4)P] and other poly-phosphoinositides (de Saint-Jean et al., 2011; Ghai et al., 2017). In the case of OSBP, PI(4)P is the preferred ligand, suggesting that both sterol and PI(4)P are transported at MCSs. *In vitro*, OSBP bridges the ER and Golgi by association with vesicle-associated membrane protein-associated protein (VAP) via the FFAT motif, and PI(4)P and Arf1 via the PH domain, respectively, to mediate the countercurrent exchange of PI(4)P and cholesterol (Mesmin et al., 2013). Pharmacological inhibition of endogenous OSBP indicates that its cholesterol transfer activity may catalyze the consumption of one-half of cellular PI(4)P and the bulk of Golgi-associated PI(4)P (Mesmin et al., 2017). Through localized changes in the sterol and PI(4)P content of ER–Golgi MCSs, OSBP also regulates the recruitment of other proteins involved in lipid transport and synthesis, such as ceramide transfer protein (CERT) and Nir2 (Peretti et al., 2008; Perry and Ridgway, 2006).

ORP4 (also known as OSBPL2) is phylogenetically related to and physically interacts with OSBP, and binds sterols and PI(4)P via the OHD, VAP via the FFAT motif and PI(4)P via the PH domain (Charman et al., 2014; Goto et al., 2012; Wyles et al., 2007). Despite these similarities, OSBP and ORP4 appear to have dissimilar cellular functions. Unlike OSBP, the ORP4 gene *OSBPL2* encodes full-length ORP4L as well as two N-terminally truncated variants (ORP4M and ORP4S) lacking PH domains. ORP4S displays increased vimentin interaction and has higher affinity for cholesterol, suggesting an autoinhibitory role for the PH domain (Charman et al., 2014). ORP4 expression is increased in disseminated tumour cells from patients with metastatic non-haematological cancers (Fournier et al., 1999), in ras-transformed intestinal epithelial cells (Charman et al., 2014) and transformed T-cells (Zhong et al., 2016b), and is required for the proliferation of transformed and immortalized cultured cells (Charman et al., 2014; Li et al., 2016). ORP4L and OSBP bind steroidal antineoplastic agents termed ORPphilins indicative of a primary role in growth-stimulatory signalling pathways (Burgett et al., 2011). Recently, ORP4L was identified as a scaffolding protein at the PM for G-protein coupled receptors and phospholipase Cβ3 (PLCβ3) that produce inositol-1,4,5-trisphosphate (IP_3) for Ca^{2+}-dependent proliferative signalling in macrophages and transformed T-cells (Zhong et al., 2016a,b). Despite this pro-proliferative function, *Osbpl2*$^{-/-}$ mice develop normally but males have oligo-astheno-teratozoospermia, which results in infertility (Udagawa et al., 2014).

The OHD of ORP4 binds both sterols and PI(4)P, and ORP4S catalyzes the transfer of cholesterol between liposomes (Charman

Atlantic Research Center, Departments of Pediatrics and Biochemistry & Molecular Biology, Dalhousie University, Halifax, NS, Canada, B3H 4R2.

*Author for correspondence (nridgway@dal.ca)

N.D.R., 0000-0002-0441-6228

Received 10 January 2018; Accepted 6 June 2018

Journal of Cell Science (2018) 131, jcs215335. doi:10.1242/jcs.215335

et al., 2014). However, despite interacting with OSBP and having a PH domain that targets the Golgi complex (Charman et al., 2014), ORP4L has not been implicated in Golgi-specific functions. Here, we show for the first time that ORP4L differentially localizes to ER–Golgi contacts in response to OSBP activation by 25-hydroxycholesterol (25OH). Fragmentation of the Golgi and TGN, and loss of PI(4)P in early Golgi compartments of ORP4L-depleted cells indicates a role for ORP4L in PI(4)P homeostasis. In contrast, PM localization of ORP4L did not require sterol, PI(4)P or VAP, indicating a non-MCS related activity.

RESULTS

Oxysterol-dependent localization of ORP4L to the Golgi and TGN

Our lab and others reported that ORP4L is present in the cytoplasm, and on intermediate filaments and the PM of cultured cells but with no evidence of Golgi localization, even in the presence of exogenous 25OH (Charman et al., 2014; Zhong et al., 2016a). Immunostaining for ORP4L–V5 expressed in HeLa cells using a V5 monoclonal antibody revealed that the protein was diffusely localized under control conditions but was detected on perinuclear structures after 25OH treatment (Fig. 1A). Co-immunostaining of the cells with a previously characterized ORP4 antibody (against amino acids 380-463 of ORP4L; Wang et al., 2002) did not detect these perinuclear structures (Fig. 1A). Perinuclear ORP4L–V5 co-localized with TGN46 in 25OH-treated cells, as well as with TGN46 at the cell periphery (Fig. 1B). We also observed 25OH-induced co-localization of ORP4L–GFP with the *medial*/*trans*-Golgi marker GALNT2 in HeLa cells (Fig. 1C) and the TGN marker PI4KIIIβ in CHO-K1 cells (Fig. 1D). Similarly to OSBP, perinuclear Golgi localization of ORP4L–V5 was also stimulated by acutely depleting HeLa cells of cholesterol with 2.5 mM methyl-β-cyclodextrin (Fig. S1A,B). Thus C-terminal-tagged ORP4L was detected at the Golgi and TGN in 25OH-treated or sterol-depleted cells but not with a polyclonal antibody directed against an internal epitope. These experiments show for the first time that ORP4L, like its close paralogue OSBP, undergoes translocation to the Golgi and that Golgi detection is epitope dependent. This finding is consistent with the Golgi localization of the GFP-PH domain of ORP4L (Charman et al., 2014, 2017).

Golgi localization of ORP4L is regulated by ligand binding and OSBP

To investigate the role of lipid binding in the Golgi localization of ORP4L, V5-tagged versions of previously characterized sterol-binding and PI(4)P-binding mutants were constructed and expressed in cells. ORP4L-Δ501-505–V5 has a deletion in the lid of the OHD that prevents sterol binding but not PI(4)P binding (Charman et al., 2014; Wyles et al., 2007). Conversely, mutating the two histidine residues in the OHD (ORP4L-HH/AA) reduced

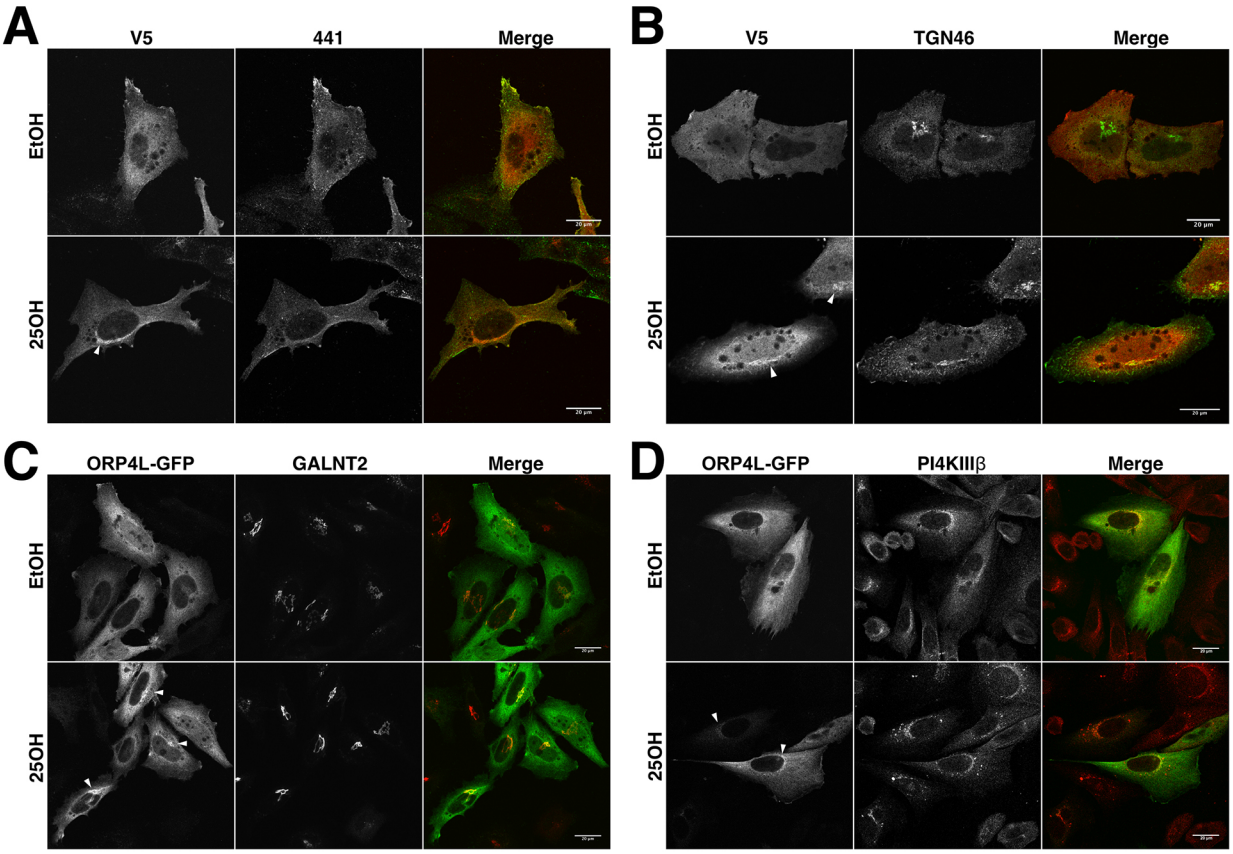

Fig. 1. Epitope-tagged ORP4L is associated with the Golgi in 25OH-treated cells. (A) HeLa cells transiently expressing ORP4L–V5 for 48 h were treated with solvent (ethanol, EtOH) or 6 µM 25OH for 2 h. Cells were then fixed, permeabilized and probed with a V5 monoclonal antibody (V5) and an ORP4 polyclonal antibody (ORP4) targeting an epitope in the central linker region, followed by Alexa Fluor-594 and -488 secondary antibodies, respectively. (B) HeLa cells were transfected and treated as described above, and probed with V5 and TGN46 antibodies, followed by Alexa Fluor-594 and -488 secondary antibodies, respectively. (C) HeLa cells transfected with ORP4L–GFP for 24 h were treated with 25OH as described above, and probed with a GALNT2 antibody followed by Alexa Fluor-594. (D) CHO-K1 cells transfected with ORP4L–GFP for 24 h and treated with 25OH as described above were probed for PI4KIIIβ and Alexa Fluor-594. Golgi structures positive for V5 antibody or GFP are indicated with arrowheads. Scale bars: 20 µm.

Journal of Cell Science (2018) 131, jcs215335. doi:10.1242/jcs.215335

binding of PI(4)P but not sterols (Charman et al., 2014; Wyles et al., 2007). To identify the role of VAP binding in recruitment to PM–ER or Golgi–ER MCSs, the FFAT motif mutant ORP4L-YF/AA–V5 was also characterized. Wild-type ORP4L–V5 was co-localized with TGN46 in 25OH-treated cells (Fig. 2A and associated line plot). Interestingly, ORP4L-Δ501-505–V5 displayed extensive TGN localization in response to 25OH (Fig. 2B), suggesting that 25OH induces a signal for ORP4L translocation that is independent of sterol binding. The association of ORP4L with the Golgi required PI(4)P and VAP binding based on the lack of TGN localization of ORP4L-HH/AA–V5 (Fig. 2C) and ORP4L-YF/AA–V5 (Fig. 2D) in 25OH-treated cells. ORP4L-Δ501-505–V5 also localized to the Golgi in response to cholesterol depletion by cyclodextrin (Fig. S1C) whereas ORP4L-HH/AA–V5 did not (Fig. S1D).

The N-terminal PH domain of ORP4L binds PI(4)P that is enriched in the Golgi (Charman et al., 2014). To determine whether ORP4L-Δ501-505–V5 localization is PI(4)P dependent, ORP4L-Δ501-505–V5 was co-expressed with wild-type, ER-restricted or Golgi-restricted mutants of Sac1, a PI(4)P phosphatase that cycles between the ER and Golgi (Blagoveshchenskaya and Mayinger, 2009). GFP–Sac1 co-localized with ORP4L-Δ501-505–V5 in 25OH-treated cells and had no effect on its appearance at the Golgi (Fig. 3A). GFP–Sac1-LZ, which does not multimerize and is constitutively in the ER, also did not affect the translocation of ORP4L-Δ501-505–V5 to the Golgi in the presence of 25OH (Fig. 3B). Expression of GFP–Sac1-K2A, a constitutive Golgi-localized mutant that reduces Golgi-associated PI(4)P (Blagoveshchenskaya et al., 2008), blocked the appearance of ORP4L-Δ501-505–V5 at the Golgi in response to 25OH (Fig. 3C). Quantification of Golgi localization revealed that expression of GFP–Sac1-K2A reduced, but did not completely prevent, the Golgi localization of ORP4L-Δ501-505–V5 (Fig. 3D). Expression of Sac1-K2A also prevented the Golgi localization of ORP4L–V5 (Fig. S2); however, 25OH-induced translocation of ORP4L was slightly less robust than the ORP4L sterol binding mutant. Thus, association of ORP4L with the Golgi depends on the Golgi pool of PI(4)P generated by 25OH treatment, which is susceptible to degradation by Sac1.

Since ORP4L and OSBP interact (Wyles et al., 2007), and OSBP regulates PI(4)P levels in the Golgi in 25OH-treated cells (Goto et al., 2016; Mesmin et al., 2013), we tested whether 25OH-mediated translocation of OSBP was required for localization of ORP4L–GFP using HeLa cells stably expressing an OSBP shRNA. HeLa shOSBP cells have significantly reduced OSBP expression relative to controls (Fig. 4C). When ORP4L–GFP was expressed in HeLa shOSBP cells, there was no evidence of perinuclear Golgi localization in the presence or absence of 25OH (Fig. 4A). However, localization of ORP4L–GFP with OSBP in the Golgi and TGN was re-established in cells expressing a shRNA-resistant OSBP cDNA (Fig. 4A). ORP4L-Δ501-505–GFP displayed weak perinuclear staining in HeLa shOSBP cells, which was enhanced when cells were transfected with the OSBP cDNA (Fig. 4B). Expression of a shRNA-resistant cDNA encoding OSBP with a deletion in the dimerization motif and leucine repeat (OSBP-Δ261-296-L313E) required for the interaction with ORP4L (Wyles et al., 2007) did not rescue sterol-induced Golgi or TGN localization of

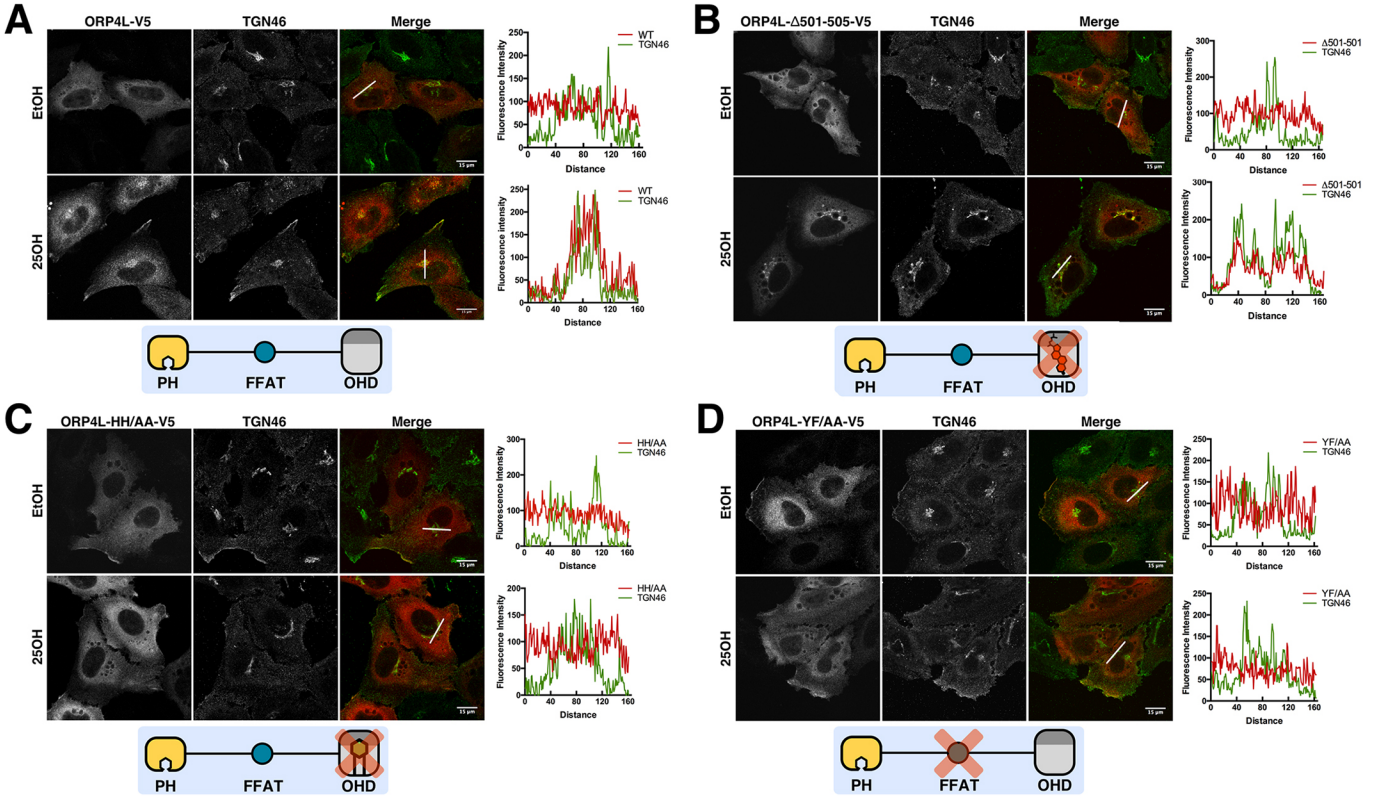

Fig. 2. Golgi localization of ORP4L is dependent on its sterol, PI(4)P and VAP binding activity. HeLa cells were transiently transfected with plasmids encoding (A) ORP4L–V5, (B) ORP4L-Δ501-505–V5, (C) ORP4L-HH/AA–V5 or (D) ORP4L-YF/AA–V5. Cells were treated with solvent (ethanol) or 6 µM 25OH for 2 h, and immunostained with V5 and TGN46 antibodies followed by Alexa Fluor-594 or -488 secondary antibodies, respectively. Images were captured by confocal microscopy (0.7 µm sections). RGB profiles for lines bisecting the TGN were created using ImageJ analysis software. The location of each functional mutation is indicated in the models below each panel. Scale bars: 15 µm.

Journal of Cell Science (2018) 131, jcs215335. doi:10.1242/jcs.215335

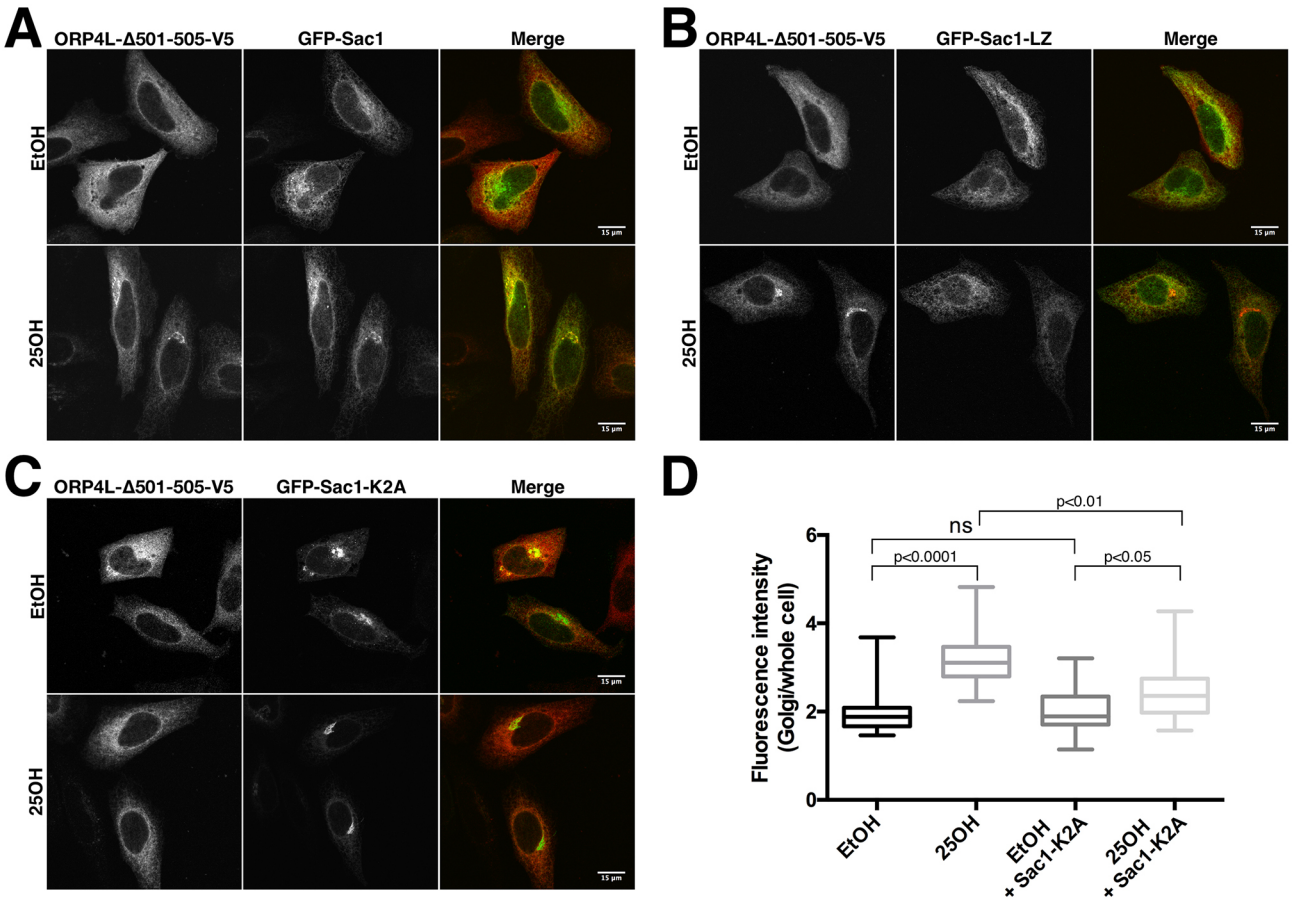

Fig. 3. Association of ORP4L-Δ501-505–V5 with the Golgi is PI(4)P dependent. HeLa cells were transiently co-transfected with vectors encoding ORP4L-Δ501-505 and (A) GFP–Sac1, (B) GFP–Sac1-LZ or (C) GFP–Sac1-K2A. After 24 h, cells were treated with solvent (ethanol) or 6 µM 25OH for 2 h and subsequently immunostained with a V5 monoclonal and Alexa Fluor-594 secondary antibody. Images were captured by confocal microscopy (0.7 µm sections). (D) The Golgi localization of ORP4L-Δ501-505–V5 was assessed in non-expressing cells and cells expressing GFP–Sac1-K2A. The localization of ORP4L-Δ501-505 to the Golgi in non-expressing controls was determined by immunostaining with TGN46 to mask the Golgi for intensity measurements. Results are shown as box and whisker plots (whiskers are 5th and 95th percentiles; box shows 25th and 75th percentiles with median) for three separate experiments (n=16–20 cells). Significance was determined by unpaired t-tests (ns, not significant). Scale bars: 15 µm.

either ORP4L–GFP or ORP4L-Δ501-505–GFP (Fig. 4A,B). This result indicates that physical interaction with OSBP is required for sterol-induced Golgi or TGN localization of ORP4L. To determine whether the enhanced Golgi association of ORP4L-Δ501-505–GFP relative to ORP4L was related to an enhanced physical interaction with OSBP, co-immunoprecipitation experiments were conducted in cells co-expressing OSBP and ORP4L–V5 or ORP4L-Δ501-505–V5 (Fig. 4D). OSBP co-immunoprecipitated with ORP4L–V5 and ORP4L-Δ501-505–V5 to a similar extent, and the interaction was independent of prior treatment of cells with 25OH. Results in Figs 3 and 4 suggest that ORP4L localization to the ER–Golgi involves a combination of physical interaction with OSBP, and provision of PI(4)P-enriched membranes as a consequence of OSBP localization to MCSs.

ORP4L regulates Golgi morphology

To assess whether ORP4L has a specific role in Golgi function, the morphology of the *cis/medial*-Golgi and TGN was visualized and quantified after silencing of ORP4L in HeLa cells using a lentiviral shRNA that targets all three isoforms (Charman et al., 2014). Compared with non-targeting controls (shNT), silencing of ORP4 caused TGN46 immunostaining to become more dispersed, with a loss of localization on the PM (Fig. 5A). Since the TGN phenotype was difficult to quantify by fluorescence intensity, maximum pixel intensity of whole-cell TGN46 staining was used as an indicator of dispersion (i.e. cells with dispersed TGN had lower maximum pixel intensities). Based on this method, a significant decrease in maximum TGN46 intensity was evident in shORP4-transduced cells (Fig. 5B). A similar decrease in intensity of GALNT2 (a *medial/trans*-Golgi marker) was also observed in shORP4-transduced HeLa cells (Fig. S3). The fluorescence intensity of giantin in the *cis/medial*-Golgi was unchanged but there was a modest, but statistically significant, reduction in the area occupied by giantin in shORP4-transduced cells (Fig. 5C). Using giantin as a mask for the *cis/medial*-Golgi, we also observed that the fluorescence intensity of PI(4)P in that compartment was reduced in both shORP4-transduced HeLa (Fig. 5D) and HEK 293 cells (Fig. 5E). Despite changes in the morphology and PI(4)P levels in Golgi compartments, the trafficking of a fluorescently labelled cholera toxin β-subunit (594-CTxB) to the Golgi was not affected (Fig. 5F,G). Thus, ORP4L is involved in maintenance of Golgi structure and PI(4)P levels, but not the retrograde trafficking of cargo from the PM to the Golgi.

Localization of OSBP at ER–Golgi MCSs in response to 25OH increases phosphatidylinositol 4-kinase IIα activity and establishes PI(4)P-enriched microdomains recognized by CERT (Banerji et al., 2010), which transports ceramide from the ER to the Golgi for

Journal of Cell Science (2018) 131, jcs215335. doi:10.1242/jcs.215335

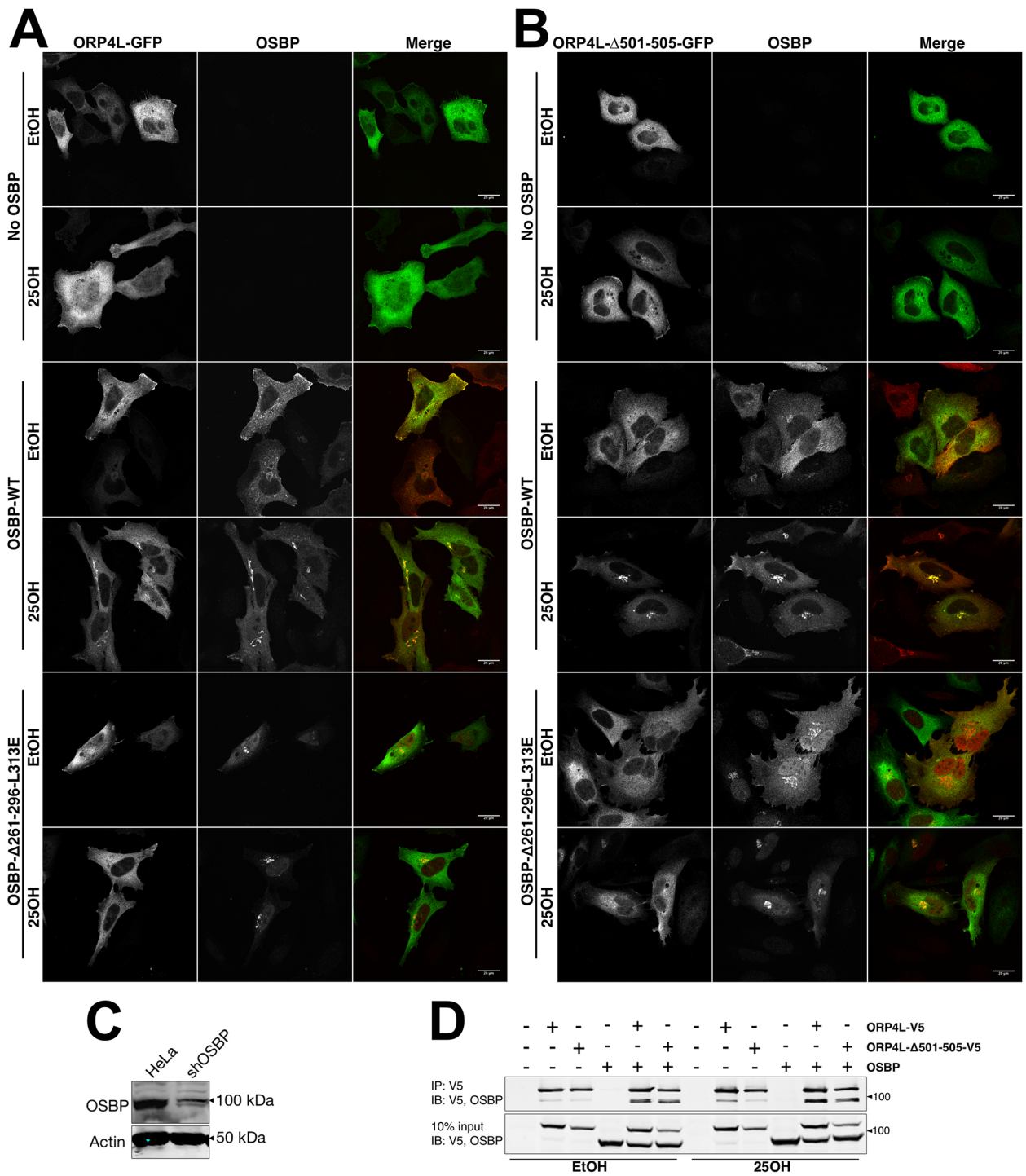

Fig. 4. Sterol-induced Golgi localization of ORP4 requires OSBP interaction. (A,B) HeLa shOSBP cells were transiently co-transfected with vectors encoding ORP4L–GFP (A) or ORP4L-Δ501-505–GFP (B) alone or in combination with shRNA-resistant OSBP or OSBP-Δ261-296-L313E. Cells were treated with ethanol or 6 µM 25OH for 2 h and subsequently probed with an OSBP monoclonal antibody followed by an Alexa Fluor-594 secondary antibody. Confocal images (0.7 µm sections) were captured. (C) Immunoblot of endogenous OSBP in HeLa cells and HeLa cells stably expressing shOSBP. (D) HeLa shOSBP cells transiently expressing ORP4L–V5 or ORP4L-Δ501-505–V5 with or without co-expression of OSBP were treated with 6 µM 25OH or solvent (ethanol) for 2 h. Cell lysates were prepared and immunoprecipitated with V5 monoclonal and probed with V5 and OSBP-monoclonal 11H9 as described in Materials and Methods. Scale bars: 20 µm.

sphingomyelin (SM) synthesis (Banerji et al., 2010; Hanada et al., 2009). To determine if ORP4 influences this OSBP activity, we measured SM synthesis in CHO-K1 cells expressing recombinant ORP4L or ORP4S. The latter served as a negative control because it does not contain the N-terminal domains necessary for interaction with OSBP or PI(4)P (Wyles et al., 2007). Expression of ORP4L or ORP4S had no effect on 25OH-activated SM synthesis mediated by OSBP (Fig. 6A). Similarly, expression of ORP4L-Δ501-505–V5 or ORP4L-HH/AA–V5, mutants that differentially interact with the Golgi (Fig. 2), had no effect on SM synthesis (Fig. 6B).

Journal of Cell Science (2018) 131, jcs215335. doi:10.1242/jcs.215335

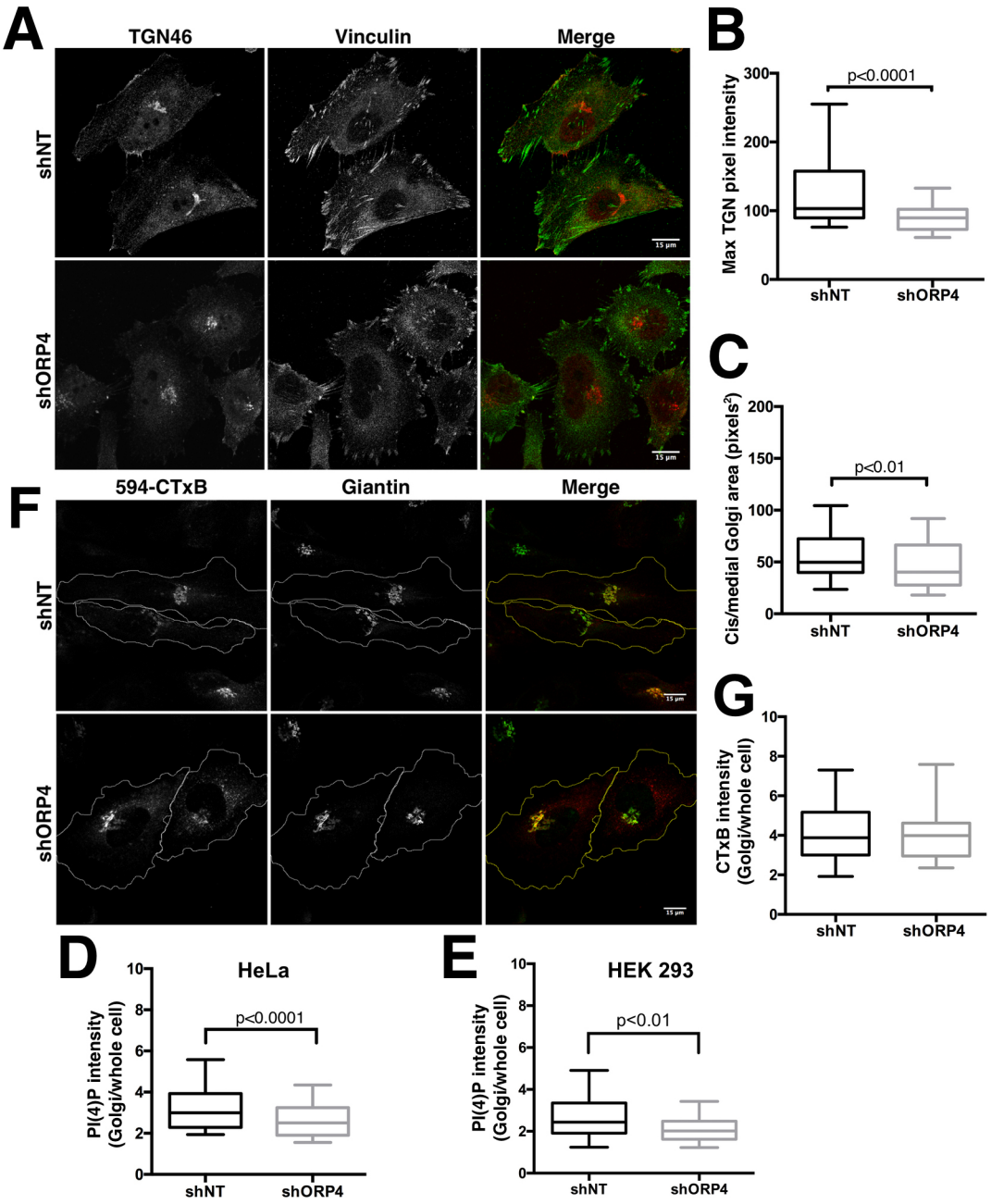

Fig. 5. ORP4 silencing affects Golgi structure and PI(4)P content. HeLa cells were transduced with lentivirus encoding non-targeting (shNT) or ORP4 shRNA (shORP4) for 24–48 h and selected in 4 µg/ml puromycin for 48 h. (A) Cells were fixed, permeabilized and probed for TGN46 and vinculin, followed by Alexa Fluor-594 and -488 secondary antibodies, respectively. (B) TGN dispersion in A was measured by maximum pixel value of the TGN46 signal (graph is representative of three experiments: shNT, 33 cells; shORP4, 50 cells). (C) The area of giantin immunofluorescence representing the *cis*/*medial*-Golgi was quantified in fixed cells from images in F. Results are from three experiments: shNT, *n*=108 cells; shOSBP, *n*=124 cells. (D,E) Using giantin as a mask for the *cis-medial*-Golgi, PI(4)P fluorescence intensity was measured in HeLa (D) and HEK 293 cells (E) as the ratio of Golgi to cytoplasmic staining. Results in D are from three experiments: shNT, *n*=195 cells; shORP4, *n*=177 cells. Results in E are from two experiments: shNT, *n*=60 cells; shORP4, *n*=54 cells. (F,G) Cells were incubated with Alexa Fluor-594-labelled cholera toxin β-subunit (CTxB) for 30 min followed by a 30 min chase period. Cells were fixed and immunostained for giantin using an Alexa Fluor-488 secondary antibody (F), which was used as a mask to quantify Golgi-localized CTxB (G). In B–E and G, results are shown as box and whisker plots (whiskers are 5th and 95th percentiles; box shows 25th and 75th percentiles with median). Significance was determined by unpaired *t*-tests. Scale bars: 15 µm.

The PM association of ORP4L does not require its VAP or lipid binding activities

In addition to sterol-dependent Golgi localization, ORP4L–V5 was observed at the plasma membrane in both control and 25OH-treated cells (see Fig. 2A). This is consistent with reports that ORP4L regulates IP_3 production by PLCβ3 at the PM, leading to release of Ca^{2+} from ER stores (Zhong et al., 2016b). Confocal imaging of HeLa cells revealed that ORP4L–V5 and the three mutants were detected at the PM under control and 25OH-treated conditions (Fig. 7A). ORP4L–V5 and the three mutants were also detected on the perimeter of cells surface-stained with 594-CTxB, confirming that the signal observed on the cell periphery is on the PM (Fig. S4).

Journal of Cell Science (2018) 131, jcs215335. doi:10.1242/jcs.215335

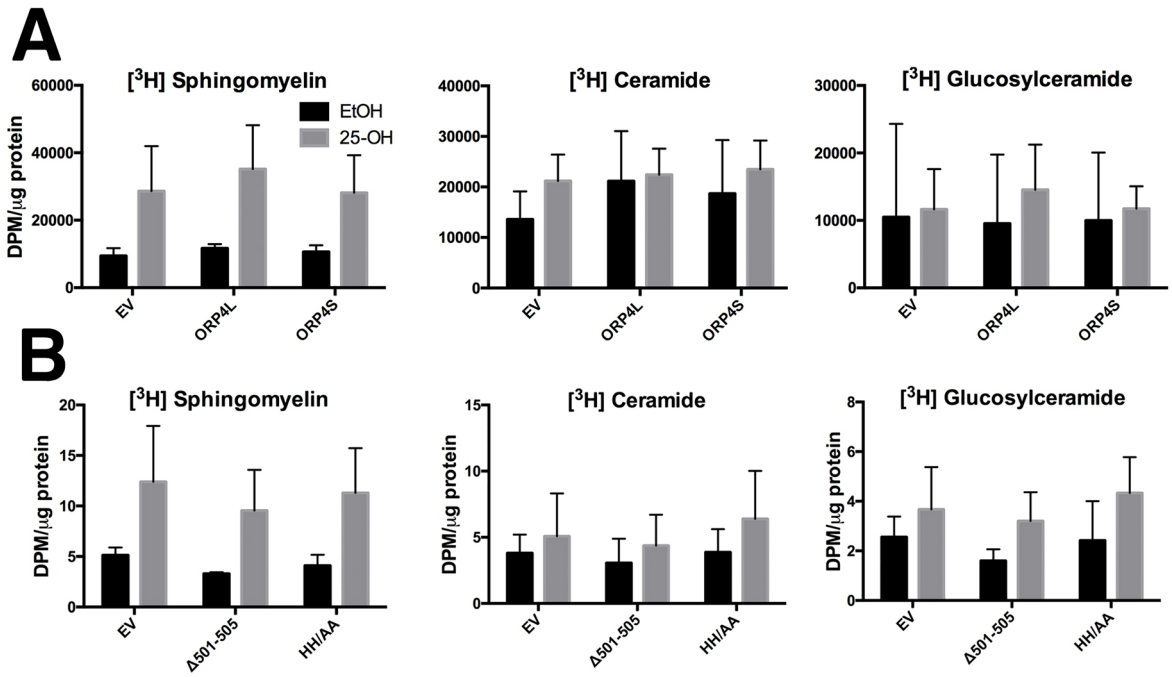

Fig. 6. ORP4 expression does not affect OSBP-dependent activation of CERT and SM synthesis. (A) CHO-K1 cells were transiently transfected with empty vector (EV), ORP4L–V5 or ORP4S–V5 and sphingomyelin, ceramide and glucosylceramide synthesis were quantified in response to ethanol (EtOH) or 25OH treatment as described in the Materials and Methods. (B) Similar experiments were repeated with CHO-K1 cells transiently expressing empty vector or ORP4L lipid binding mutants. Results are the mean±s.d. of three experiments.

Qualitative analysis of confocal images from several experiments indicated that ORP4L–V5 was detected at the PM in 60–80% of control and 25OH-treated cells, and that this PM distribution was similar for the sterol, PI(4)P or VAP binding mutants. Endogenous VAPA immunostaining extended out to the PM but did not co-localize with ORP4L–V5 or the three ORP4L mutants (Fig. 7A), indicating an absence of discrete PM–ER contacts mediated by ORP4L and VAPA. To further test whether VAPA was localized with ORP4L at the PM, ORP4L–GFP and mCherry–VAPA were co-expressed in HeLa cells and imaged at the PM by total internal reflection fluorescence (TIRF) microscopy (Fig. 7B). TIRF imaging showed a diffuse localization of ORP4L–GFP at the PM under normal and 25OH-treated conditions. mCherry–VAPA was also detected at the PM but the pattern was more reticular in nature and did not co-localize with ORP4L–GFP (Fig. 7B).

ORP4L–V5 co-localized with and was regulated by Golgi-associated PI(4)P (Figs 3 and 5). To determine whether ORP4L is targeted to regions of the PM containing PI(4)P, localization of ORP4L–GFP with the PI(4)P sensor mCherry–SidM (Hammond et al., 2014) was determined by TIRF imaging (Fig. 8A). ORP4L–GFP was co-localized with diffuse and concentrated regions of mCherry–SidM under control and 25OH-treated conditions. In comparison, ORP4L–GFP did not co-localize with puncta labelled with the mCherry-tagged PH domain of PLCδ, a $PI(4,5)P_2$ sensor (Stauffer et al., 1998; Várnai and Balla, 1998) (Fig. 8B). Thus, association of ORP4L with the PM was independent of its lipid and VAP binding activities, but coincided with PI(4)P-positive regions of the membrane.

DISCUSSION

Members of the OSBP/ORP family form bridges between organelles at MCSs via the protein and lipid binding activities of their PH, FFAT and ankyrin motifs. Increasingly, ORPs are found to be active at more than one organelle and MCS. For example, ORP5 transfers lipids or regulates metabolism at MCSs between the ER and late endosome (Du et al., 2011), the ER and mitochondria (Galmes et al., 2016) and the ER and PM (Chung et al., 2015). The organelle localization and activity of ORP4L is also heterogeneous. An essential proliferative function of ORP4L is the regulation of Ca^{2+} homeostasis via scaffolding of PLCβ3 and production of IP_3 at the PM (Zhong et al., 2016a,b). However, ORP4L is also localized to the cytoplasm and interacts with the intermediate filament protein vimentin (Wang et al., 2002). In addition, we show that the OSBP, lipid and VAP binding activities of ORP4L control its association at the ER–Golgi interface where it influences PI(4)P content and structure of the TGN and proximal Golgi compartments.

Prior studies from our lab utilized an antibody that recognized an internal epitope in ORP4L that did not detect the Golgi-associated protein, possibly due to epitope masking in ORP4L that associated with the Golgi. In contrast, C-terminal epitope-tagged ORP4L clearly associated with the Golgi and TGN in cells treated with 25OH or after cholesterol depletion with cyclodextrin, treatments that also cause OSBP to translocate to ER–Golgi contact sites (Ridgway et al., 1998). The detection of ORP4L at the Golgi reconciles previous reports of Golgi localization of the ORP4L GFP-PH domain and the presence of the ORP4L-interacting partner OSBP at ER–Golgi MCSs. Direct sterol binding to ORP4L does not mediate translocation since ORP4L-Δ501-505–V5, a sterol-binding defective mutant that retained PI(4)P binding activity, moved to the TGN in response to 25OH and cyclodextrin. Rather, association of ORP4L and ORP4L-Δ501-505–V5 with the Golgi or TGN was dependent on OSBP and a Sac1-regulated pool of PI(4)P in the Golgi. OSBP could activate ORP4L localization to the ER–Golgi by two mechanisms. First, OSBP activation by 25OH increases a pool of Golgi PI(4)P that is specifically recognized by the GFP-PH domain of ORP4L (Charman et al., 2017). It follows that the

Journal of Cell Science (2018) 131, jcs215335. doi:10.1242/jcs.215335

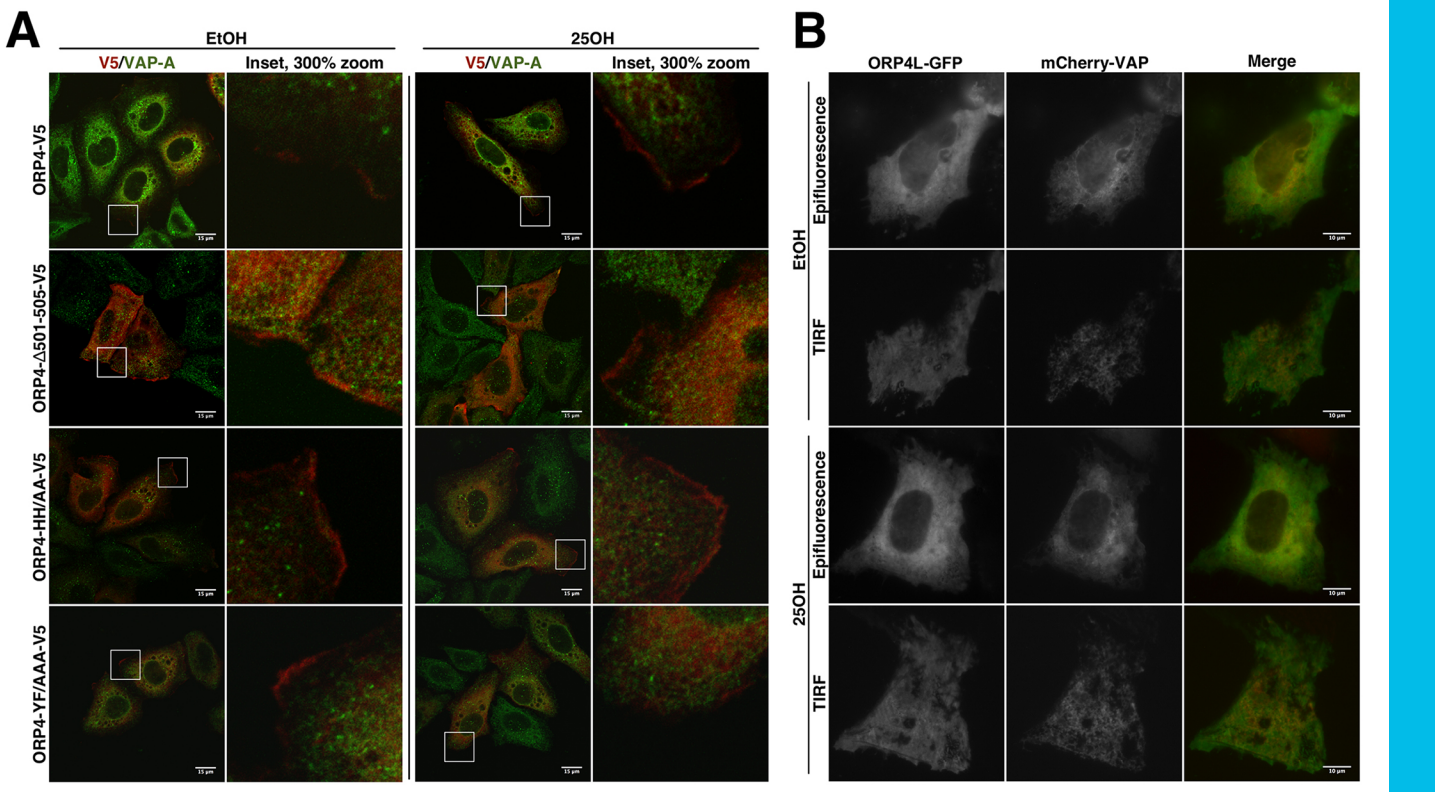

Fig. 7. ORP4L–V5 partially localizes to the plasma membrane. (A) HeLa cells were transiently transfected with constructs encoding ORP4L, ORP4L-Δ501-505–V5, ORP4L-HH/AA–V5 or ORP4L-YF/AA–V5. Cells were incubated for 2 h in ethanol or 6 µM 25OH, followed by immunostaining with V5 and VAPA primary antibodies and Alexa Fluor-594 and -488 secondary antibodies, respectively. Images were captured by confocal imaging (0.7 µm sections). Note that the absence of Golgi staining in 25OH-treated cells expressing ORP4L and ORP4L-Δ501-505 is due to optimization of the focal plane to visualize PM staining rather than internal structures. (B) HeLa cells cultured on glass-bottom dishes were transiently transfected with ORP4L–GFP and mCherry–VAP constructs, and images were captured by TIRF microscopy before and after a 2 h treatment with 6 µM 25OH. Scale bars: 15 µm.

degradation of this PI(4)P pool by overexpression of the Golgi-localized Sac1-K2A mutant accounts for attenuation of ORP4L–V5 recruitment to the TGN. Second, there could be a direct physical interaction that increases ORP4L recruitment to ER–Golgi MCSs that contain OSBP. Initial interaction with OSBP would then facilitate binding of ORP4L to PI(4)P and VAP, thus stabilizing its interaction at MCSs. This concept is supported by the finding that an OSBP mutant (OSBP-Δ261-296-L313E) that does not interact with ORP4L also failed to rescue Golgi and TGN localization of either ORP4L or ORP4L-Δ501-505 in shOSBP cells.

Since ORP4L-YF/AA–V5 did not move to the Golgi in response to 25OH, ORP4L likely localizes to ER–Golgi MCSs through interaction with VAP in the ER. Since ORP4L binds cholesterol and PI(4)P and mediates cholesterol transfer *in vitro* (Charman et al., 2014), it could transfer these lipids at an MCS in parallel or in opposition to OSBP. Since ORP4L-Δ501-505–V5 localized to ER–Golgi MCSs but the PI(4)P binding mutant ORP4L-HH/AA–V5 did not, it appears that PI(4)P binding is a required step in ORP4L recruitment to MCSs that harbour OSBP. We ruled out a potential role for ORP4L in OSBP-dependent sphingolipid synthesis, indicating that ORP4L functions downstream of OSBP, perhaps as a recruited factor at MCSs like CERT and Nir2. Both of these proteins also transfer lipids at MCSs, suggesting ORP4L might have a similar function.

The results of silencing experiments indicate a role for ORP4L in the maintenance of Golgi structure, possibly by a PI(4)P-dependent mechanism. This conclusion is also supported by imaging studies of cells treated with ORPphilins, which bind and inhibit both OSBP and ORP4L (Burgett et al., 2011). Cell death and morphological defects in the Golgi caused by ORPphilins were evident in cells with OSBP knockdown, suggesting that ORP4L was the primary mediator of drug effects. It is currently unknown if Golgi–ER-specific activities of ORP4L contribute to its proliferative and growth promoting properties or whether they are secondary phenomena. The Golgi and TGN dispersion phenotype of ORP4L silencing could be secondary to effects on other interacting factors since aberrant PI(4)P metabolism in the Golgi (Liu et al., 2009), as well as knockdown of VAP and OSBP (Nishimura et al., 2013; Peretti et al., 2008), cause a Golgi dispersion phenotype.

The presence of ORP4L at the PM in HeLa cells is consistent with its recently discovered regulation of IP_3 production and ER Ca^{2+} release via PLCβ3 regulation (Zhong et al., 2016b). We observed that the PM localization of ORP4L was independent of VAP binding activity that controlled its association with the ER–Golgi MCSs. This result is consistent with the observation that VAP binding was not required for the PLCβ3 scaffolding activity of ORP4L (Zhong et al., 2016b), indicating that PM–ER MCSs are not involved. TIRF imaging showed that ORP4L was localized at the PM with the PI(4)P sensor SidM. Again, this agrees with the requirement for the ORP4L PH domain, which recognizes PI(4)P *in vitro* (Charman et al., 2014), for PLCβ3 scaffolding (Zhong et al., 2016b). However, the ORP4L GFP-PH domain was not detected at the PM (Charman et al., 2014), indicating the involvement of other domains in the PM targeting of ORP4L. We excluded a role for OHD lipid binding since both ORP4L-HH/AA–V5 and ORP4L-Δ501-505–V5 were present on the PM. We conclude that ORP4L

Journal of Cell Science (2018) 131, jcs215335. doi:10.1242/jcs.215335

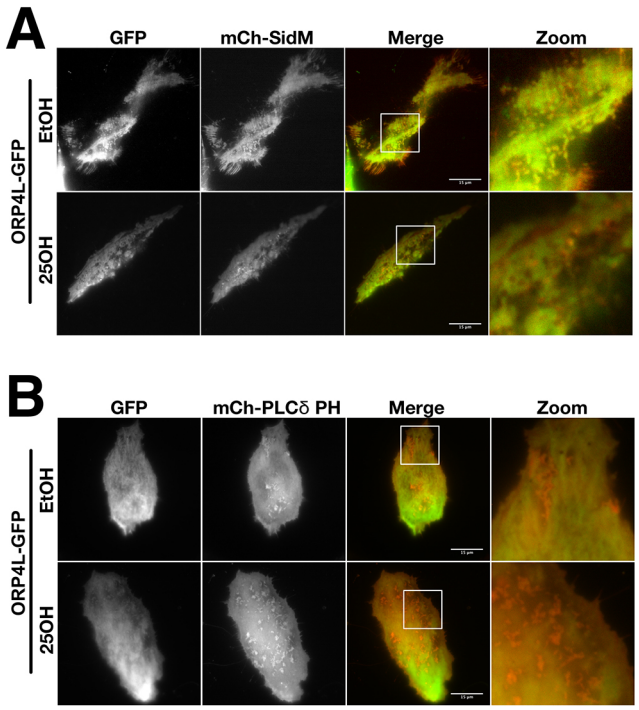

Fig. 8. TIRF imaging of ORP4L with sensors for PI(4)P and PI(4,5)P_2. HeLa cells cultured on glass-bottom dishes were transiently transfected with vectors encoding ORP4L–GFP and (A) mCherry–SidM or (B) mCherry–PLCδ-PH. Cells were subsequently treated with either ethanol or 6 µM 25OH for 2 h followed by TIRF imaging as described in Materials and Methods. Scale bars: 15 µm.

could have two independently regulated activities: one at the PM related to cell signalling, the other that controls lipid transport or metabolism at ER–Golgi MCSs that is critical for organelle morphology.

MATERIALS AND METHODS

Antibodies and plasmids

The following antibodies were used for both western blotting and immunofluorescence at the indicated dilutions: TGN46 (Bethyl Laboratories, A304-434, 1:2000 dilution), vinculin (Abcam, Ab130007, 1:500), GALNT2 (Biolegend, #682302, 1:1000 dilution), PI4KIIIβ (BD Biosciences #611816, 1:500), giantin (BioLegend, #19243, 1:2000), PI(4)P (Echelon, ZP004, 1:1000 dilution), VAPA (1:1000 dilution; Wyles et al., 2002) and V5 (Bio-Rad, 1:2000 dilution), affinity-purified rabbit polyclonal against amino acids 380-473 of ORP4L (1:1000 dilution; Wang et al., 2002), and OSBP monoclonal 11H9 (1:100 dilution; Ridgway et al., 1992). For western blotting, a polyclonal antibody against OSBP (Ridgway et al., 1992; Wyles and Ridgway, 2004) was used at a 1:10,000 dilution. Secondary IRDye 800CW- and IRDye 680LT-conjugated antibodies (LI-COR Biosciences, 1:15,000 and 1:20,000 dilution, respectively) and Alexa Fluor 488- and 594-conjugated antibodies (Molecular Probes, 1:5000 dilution) were used for immunoblotting and immunofluorescence, respectively.

An shRNA-resistant ORP4L cDNA in pcDNA 3.1 V5-His (ORP4L–V5) was used as a template to mutagenize histidines 589 and 590 to alanine (ORP4L-HH/AA–V5), Y415 and F416 to alanine (ORP4L-YF/AA–V5) and to create a deletion of amino acids 501–505 (ORP4L-Δ501-505–V5). Mutations were confirmed by sequencing. pORP4L–GFP was prepared by restriction digestion of ORP4L–V5-His and ligation into pEGFP-N1. Lentivirus was prepared using pLKO.1 constructs encoding non-targeting shRNA (shNT; CAA CAA GAT GAA GAG CAC AAC) or an shRNA targeting all three ORP4 isoforms (shORP4; CAT CAC ATC CAA TGC TAT GAT).

Cell culture, transfection and transduction

HeLa and HEK 293T cells (from ATCC) were cultured in DMEM supplemented with 10% (v/v) FBS (Medium A). CHO-KI cells (from ATCC) were cultured in DMEM supplemented with 35 µg/ml proline, 5% (v/v) FCS and blasticidin (2 mg/ml). HeLa cells stably expressing the lentiviral shOSBP were cultured in Medium A with blasticidin (2 mg/ml). Transient transfection of plasmids was performed with Lipofectamine 2000 (Invitrogen).

Quantification of sphingomyelin synthesis

Transfected CHO-K1 cells were incubated for 4 h with 6 µM 25OH or solvent control (ethanol). During the final 2 h of treatment, sphingolipid synthesis was quantified by pulse-labelling with [^{3}H]serine (10 µCi/ml) (Ridgway, 1995). Cells were harvested in methanol:water (5:4, v/v), lipids were extracted from cell lysates with chloroform:methanol (1:2) and 0.58% NaCl, and the chloroform phase was washed twice with methanol:58% NaCl:chloroform (45:47:3, v/v). Radiolabelled glycerolipids were hydrolysed in 0.1 N KOH for 1 h at 37°C and the resultant sphingolipid fraction was resolved by thin-layer chromatography (TLC) in chloroform: methanol:water (65:25:4 v/v). Radioactivity in SM, ceramide and glucosylceramide was quantified by scraping TLC plates and liquid scintillation counting (Fig. 6A), or by direct radiometric scanning of TLC plates using an AR2000 Scanner and WinScan software v3.14 (Eckert & Ziegler Radiopharma, Hopkinton, MA) (Fig. 6B). [^{3}H]Serine incorporation into lipids was expressed relative to total cell protein.

Immunoprecipitation and immunoblotting

Cells were rinsed with PBS, scraped and sedimented by low-speed centrifugation. Cell pellets were lysed on ice for 15 min in 0.1 ml of HEPES lysis buffer (25 mM HEPES, 150 mM NaCl, 2 mM EDTA, pH 7.4) supplemented with EDTA-free protease inhibitor cocktail (Sigma-Aldrich). Detergent-insoluble material was removed by centrifugation at 4°C, supernatants were incubated with appropriate antibodies on ice for 2 h, and then combined at 4°C with Protein A–Sepharose. After 30 min, Sepharose beads were washed three times with the appropriate lysis buffer, eluted in 2.5× SDS-PAGE buffer and heated at 95°C for 5 min. Samples were resolved by SDS-PAGE, transferred to nitrocellulose membranes and blocked in a 4:1 mixture of Tris-buffered saline (TBS; 50 mM Tris-HCl, 150 mM NaCl, pH 7.4) and Odyssey blocking buffer (LI-COR Biosciences). Subsequent antibody incubations were performed in 4:1 TBS with 0.1% (v/v) Tween-20 detergent and Odyssey blocking buffer. Antibody binding was visualized using the LI-COR Odyssey infrared imaging system and associated secondary antibodies.

Immunofluorescence and TIRF microscopy

Immunocytochemical detection of PI(4)P in the Golgi was performed as previously described (Hammond et al., 2009). Briefly, cells cultured on glass coverslips were fixed with 2% formaldehyde in PBS for 10 min at ambient temperature, quenched with 50 mM ammonium chloride and permeabilized for 20 min at ambient temperature with 15 µg/ml digitonin in 100 mM glycine. Cells were blocked for 1 h with PBS containing 1% BSA (w/v), incubated with a PI(4)P antibody (16 h), an Alexa Fluor-labelled secondary antibody and mounted in Mowiol 40-88. For all other indirect immunofluorescence microscopy, cells cultured on glass coverslips were fixed with 4% (w/v) paraformaldehyde in PBS for 12 min at ambient temperature, quenched with 50 mM ammonium chloride and permeabilized for 12 min at 4°C with Triton X-100 (0.05%, w/v) in PBS. Permeabilized cells were blocked with PBS containing 1% BSA (w/v) and probed with primary and secondary antibodies diluted in the same buffer. Cells were rinsed with distilled water prior to mounting in Mowiol 40-88. For cell surface staining with 594-CTxB, cells incubated at 4°C for 1 h were probed with 594-CTxB (1 µg/ml) on ice for 75 min, then washed with cold PBS prior to paraformaldehyde fixation, Triton X-100 permeabilization and antibody probing as described above. Confocal immunofluorescence microscopy was performed on a Zeiss LSM 510 laser-scanning confocal microscope with Zen acquisition software. Image analysis was performed using ImageJ software v.1.49.

For TIRF microscopy, cells were cultured on dishes with #1.5 coverglass (170 µm) bottoms. Following transfection of cDNAs encoding GFP- and mCherry-tagged proteins for 24 h, cells were mounted on the environmentally controlled stage of a Zeiss Cell Observer spinning-disk confocal microscope. TIRF images were captured at an incident angle of 67° with a 100× oil-immersion objective (NA 1.45), and epifluorescence images were taken after resetting the incident angle to 0°.

Acknowledgements
We thank Robert Douglas for technical assistance with tissue culture and Stephen Whitefield for assistance with TIRF microscopy.

Competing interests
The authors declare no competing or financial interests.

Author contributions
Conceptualization: N.D.R.; Methodology: A.P., N.D.R.; Validation: A.P., N.D.R.; Formal analysis: A.P.; Investigation: A.P.; Data curation: A.P., N.D.R.; Writing - original draft: A.P., N.D.R.; Writing - review & editing: A.P., N.D.R.; Supervision: N.D.R.; Project administration: N.D.R.; Funding acquisition: N.D.R.

Funding
Funding was received from the Canadian Institutes of Health Research (MOP-15284) and the Bernard and Winnifred Mary Lockwood Endowment Fund.

Supplementary information
Supplementary information available online at
http://jcs.biologists.org/lookup/doi/10.1242/jcs.215335.supplemental

References
Banerji, S., Ngo, M., Lane, C. F., Robinson, C.-A., Minogue, S. and Ridgway, N. D. (2010). Oxysterol binding protein-dependent activation of sphingomyelin synthesis in the Golgi apparatus requires phosphatidylinositol 4-kinase IIα. *Mol. Biol. Cell* **21**, 4141-4150.

Blagoveshchenskaya, A., Cheong, F. Y., Rohde, H. M., Glover, G., Knödler, A., Nicolson, T., Boehmelt, G. and Mayinger, P. (2008). Integration of Golgi trafficking and growth factor signaling by the lipid phosphatase SAC1. *J. Cell Biol.* **180**, 803-812.

Blagoveshchenskaya, A. and Mayinger, P. (2009). SAC1 lipid phosphatase and growth control of the secretory pathway. *Mol. BioSyst.* **5**, 36-42.

Burgett, A. W. G., Poulsen, T. B., Wangkanont, K., Anderson, D. R., Kikuchi, C., Shimada, K., Okubo, S., Fortner, K. C., Mimaki, Y., Kuroda, M. et al. (2011). Natural products reveal cancer cell dependence on oxysterol-binding proteins. *Nat. Chem. Biol.* **7**, 639-647.

Charman, M., Colbourne, T. R., Pietrangelo, A., Kreplak, L. and Ridgway, N. D. (2014). Oxysterol-binding protein (OSBP)-related protein 4 (ORP4) is essential for cell proliferation and survival. *J. Biol. Chem.* **289**, 15705-15717.

Charman, M., Goto, A. and Ridgway, N. D. (2017). Oxysterol-binding protein recruitment and activity at the endoplasmic reticulum-Golgi interface are independent of Sac1. *Traffic* **18**, 519-529.

Chung, J., Torta, F., Masai, K., Lucast, L., Czapla, H., Tanner, L. B., Narayanaswamy, P., Wenk, M. R., Nakatsu, F. and De Camilli, P. (2015). PI4P/phosphatidylserine countertransport at ORP5- and ORP8-mediated ER-plasma membrane contacts. *Science* **349**, 428-432.

Dawson, P. A., Van der Westhuyzen, D. R., Goldstein, J. L. and Brown, M. S. (1989). Purification of oxysterol binding protein from hamster liver cytosol. *J. Biol. Chem.* **264**, 9046-9052.

de Saint-Jean, M., Delfosse, V., Douguet, D., Chicanne, G., Payrastre, B., Bourguet, W., Antonny, B. and Drin, G. (2011). Osh4p exchanges sterols for phosphatidylinositol 4-phosphate between lipid bilayers. *J. Cell Biol.* **195**, 965-978.

Du, X., Kumar, J., Ferguson, C., Schulz, T. A., Ong, Y. S., Hong, W., Prinz, W. A., Parton, R. G., Brown, A. J. and Yang, H. (2011). A role for oxysterol-binding protein-related protein 5 in endosomal cholesterol trafficking. *J. Cell Biol.* **192**, 121-135.

Fournier, M. V., Guimaraes da Costa, F., Paschoal, M. E., Ronco, L. V., Carvalho, M. G. and Pardee, A. B. (1999). Identification of a gene encoding a human oxysterol-binding protein- homologue: a potential general molecular marker for blood dissemination of solid tumors. *Cancer Res.* **59**, 3748-3753.

Galmes, R., Houcine, A., van Vliet, A. R., Agostinis, P., Jackson, C. L. and Giordano, F. (2016). ORP5/ORP8 localize to endoplasmic reticulum-mitochondria contacts and are involved in mitochondrial function. *EMBO Rep.* **17**, 800-810.

Ghai, R., Du, X., Wang, H., Dong, J., Ferguson, C., Brown, A. J., Parton, R. G., Wu, J.-W. and Yang, H. (2017). ORP5 and ORP8 bind phosphatidylinositol-4, 5-biphosphate (PtdIns(4,5)P 2) and regulate its level at the plasma membrane. *Nat. Commun.* **8**, 757.

Goto, A., Liu, X., Robinson, C. A. and Ridgway, N. D. (2012). Multisite phosphorylation of oxysterol-binding protein regulates sterol binding and activation of sphingomyelin synthesis. *Mol. Biol. Cell* **23**, 3624-3635.

Goto, A., Charman, M. and Ridgway, N. D. (2016). Oxysterol-binding protein activation at endoplasmic reticulum-Golgi contact sites reorganizes phosphatidylinositol 4-phosphate pools. *J. Biol. Chem.* **291**, 1336-1347.

Hammond, G. R. V., Schiavo, G. and Irvine, R. F. (2009). Immunocytochemical techniques reveal multiple, distinct cellular pools of PtdIns4P and PtdIns(4,5)P(2). *Biochem. J.* **422**, 23-35.

Hammond, G. R. V., Machner, M. P. and Balla, T. (2014). A novel probe for phosphatidylinositol 4-phosphate reveals multiple pools beyond the Golgi. *J. Cell Biol.* **205**, 113-126.

Hanada, K., Kumagai, K., Tomishige, N. and Yamaji, T. (2009). CERT-mediated trafficking of ceramide. *Biochim. Biophys. Acta* **1791**, 684-691.

Jansen, M., Ohsaki, Y., Rita Rega, L., Bittman, R., Olkkonen, V. M. and Ikonen, E. (2011). Role of ORPs in sterol transport from plasma membrane to ER and lipid droplets in mammalian cells. *Traffic* **12**, 218-231.

Li, J. W., Xiao, Y. L., Lai, C. F., Lou, N., Ma, H. L., Zhu, B. Y., Zhong, W. B. and Yan, D. G. (2016). Oxysterol-binding protein-related protein 4L promotes cell proliferation by sustaining intracellular Ca2+ homeostasis in cervical carcinoma cell lines. *Oncotarget* **7**, 65849-65861.

Liu, Y., Boukhelifa, M., Tribble, E. and Bankaitis, V. A. (2009). Functional studies of the mammalian Sac1 phosphoinositide phosphatase. *Adv. Enzyme Regul.* **49**, 75-86.

Mesmin, B., Bigay, J., Moser von Filseck, J., Lacas-Gervais, S., Drin, G. and Antonny, B. (2013). A four-step cycle driven by PI(4)P hydrolysis directs sterol/PI(4)P exchange by the ER-Golgi tether OSBP. *Cell* **155**, 830-843.

Mesmin, B., Bigay, J., Polidori, J., Jamecna, D., Lacas-Gervais, S. and Antonny, B. (2017). Sterol transfer, PI4P consumption, and control of membrane lipid order by endogenous OSBP. *EMBO J.* **36**, 3156-3174.

Ngo, M. H., Colbourne, T. R. and Ridgway, N. D. (2010). Functional implications of sterol transport by the oxysterol-binding protein gene family. *Biochem. J.* **429**, 13-24.

Nishimura, T., Uchida, Y., Yachi, R., Kudlyk, T., Lupashin, V., Inoue, T., Taguchi, T. and Arai, H. (2013). Oxysterol-binding protein (OSBP) is required for the perinuclear localization of intra-Golgi v-SNAREs. *Mol. Biol. Cell* **24**, 3534-3544.

Olkkonen, V. M. and Li, S. (2013). Oxysterol-binding proteins: sterol and phosphoinositide sensors coordinating transport, signaling and metabolism. *Prog. Lipid Res.* **52**, 529-538.

Peretti, D., Dahan, N., Shimoni, E., Hirschberg, K. and Lev, S. (2008). Coordinated lipid transfer between the endoplasmic reticulum and the Golgi complex requires the VAP proteins and is essential for Golgi-mediated transport. *Mol. Biol. Cell* **19**, 3871-3884.

Perry, R. J. and Ridgway, N. D. (2006). Oxysterol-binding protein and vesicle-associated membrane protein-associated protein are required for sterol-dependent activation of the ceramide transport protein. *Mol. Biol. Cell* **17**, 2604-2616.

Ridgway, N. D. (1995). 25-Hydroxycholesterol stimulates sphingomyelin synthesis in Chinese hamster ovary cells. *J. Lipid Res.* **36**, 1345-1358.

Ridgway, N. D., Dawson, P. A., Ho, Y. K., Brown, M. S. and Goldstein, J. L. (1992). Translocation of oxysterol binding protein to Golgi apparatus triggered by ligand binding. *J. Cell Biol.* **116**, 307-319.

Ridgway, N. D., Lagace, T. A., Cook, H. W. and Byers, D. M. (1998). Differential effects of sphingomyelin hydrolysis and cholesterol transport on oxysterol-binding protein phosphorylation and Golgi localization. *J. Biol. Chem.* **273**, 31621-31628.

Stauffer, T. P., Ahn, S. and Meyer, T. (1998). Receptor-induced transient reduction in plasma membrane PtdIns(4,5)P2 concentration monitored in living cells. *Curr. Biol.* **8**, 343-346.

Udagawa, O., Ito, C., Ogonuki, N., Sato, H., Lee, S., Tripvanuntakul, P., Ichi, I., Uchida, Y., Nishimura, T., Murakami, M. et al. (2014). Oligo-astheno-teratozoospermia in mice lacking ORP4, a sterol-binding protein in the OSBP-related protein family. *Genes Cells* **19**, 13-27.

van der Kant, R., Fish, A., Janssen, L., Janssen, H., Krom, S., Ho, N., Brummelkamp, T., Carette, J., Rocha, N. and Neefjes, J. (2013). Late endosomal transport and tethering are coupled processes controlled by RILP and the cholesterol sensor ORP1L. *J. Cell Sci.* **126**, 3462-3474.

Várnai, P. and Balla, T. (1998). Visualization of phosphoinositides that bind pleckstrin homology domains: calcium- and agonist-induced dynamic changes and relationship to myo-[3H]inositol-labeled phosphoinositide pools. *J. Cell Biol.* **143**, 501-510.

Wang, C., JeBailey, L. and Ridgway, N. D. (2002). Oxysterol-binding-protein (OSBP)-related protein 4 binds 25-hydroxycholesterol and interacts with vimentin intermediate filaments. *Biochem. J.* **361**, 461-472.

Wang, P.-Y., Weng, J., Lee, S. and Anderson, R. G. W. (2008). The N terminus controls sterol binding while the C terminus regulates the scaffolding function of OSBP. *J. Biol. Chem.* **283**, 8034-8045.

Wong, L. H., Čopič, A. and Levine, T. P. (2017). Advances on the transfer of lipids by lipid transfer proteins. *Trends Biochem. Sci.* **42**, 516-530.

Wyles, J. P. and Ridgway, N. D. (2004). VAMP-associated protein-A regulates partitioning of oxysterol-binding protein-related protein-9 between the endoplasmic reticulum and Golgi apparatus. *Exp. Cell Res.* **297**, 533-547.

Wyles, J. P., McMaster, C. R. and Ridgway, N. D. (2002). Vesicle-associated Membrane Protein-associated Protein-A (VAP-A) Interacts with the Oxysterol-binding Protein to Modify Export from the Endoplasmic Reticulum. *J. Biol. Chem.* **277**, 29908-29918.

Wyles, J. P., Perry, R. J. and Ridgway, N. D. (2007). Characterization of the sterol-binding domain of oxysterol-binding protein (OSBP)-related protein 4 reveals a novel role in vimentin organization. *Exp. Cell Res.* **313**, 1426-1437.

Zhao, K. and Ridgway, N. D. (2017). Oxysterol-binding protein-related protein 1L regulates cholesterol egress from the endo-lysosomal system. *Cell Rep.* **19**, 1807-1818.

Zhong, W., Pan, G., Wang, L., Li, S., Ou, J., Xu, M., Li, J., Zhu, B., Cao, X., Ma, H. et al. (2016a). ORP4L facilitates macrophage survival via G-protein-coupled signaling: ORP4L−/− mice display a reduction of atherosclerosis. *Circ. Res.* **119**, 1296-1312.

Zhong, W., Yi, Q., Xu, B., Li, S., Wang, T., Liu, F., Zhu, B., Hoffmann, P. R., Ji, G., Lei, P. et al. (2016b). ORP4L is essential for T-cell acute lymphoblastic leukemia cell survival. *Nat. Commun.* **7**, 12702.